Energy Equip. Sys./ Vol. 6/No. 1/March 2018/ 7-15

ENERGY EQUIPSYS

Energy Equipment and Systems

http://energyequipsys.ut.ac.ir
www.energyequipsys.com

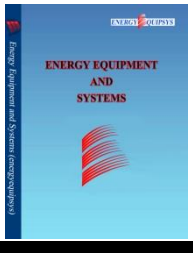

Drag coefficient and strouhal number analysis of a rectangular probe in a two-phase cross flow

Authors

Erfan Kosari[a]*
Ali Rahnama[b]
Mahyar Momen[c]
Pedram Hanafizadeh[b]
Mohammad Mahdi Rastegardoost [b]

[a] Mechanical Engineering Department, University of California, Riverside, CA, USA

[b] School of Mechanical Engineering, University of Tehran, Tehran, Iran

[c] School of Mechanical Engineering, KNT, University of Technology, Tehran, Iran

Article history:

Received : 31 July 2017
Accepted : 6 January 2018

ABSTRACT

In some case of laboratory and industrial applications, various kind of measurement instruments must be placed in a conduit, in which multiphase fluid flows. Vortex shedding for any immersed body in flow field is created with a frequency, which according to flow conditions such as flow rates, geometry of body, etc. may be constant or variable. Failure may happen, if this frequency is close to one of the natural frequencies of the instruments. These flows can play a significant role in long-term reliability and safety of industrial and laboratory systems. In this study, an Eulerian–Eulerian approach is employed to simulate Air-Water two-phase flow around a rectangular probe with different volume fractions (0.01-0.5) and Reynolds numbers (1000-3000). Two-phase flow characteristics around the probe have been analyzed numerically. The results show vortex shedding in all cases with distinct Strouhal number. In addition, results illustrate that shedding is intensified by increasing Reynolds number. In order to validate the results, fraction of inlet volume was set to zero, and drag coefficient and its relation with low Reynolds number (1000-3000) in single phase flow were compared to experimental and numerical results in published article. The results show a complete agreement between the simulation and available data.

Keywords: Two-Phase Cross Flow, Strouhal Number, Rectangular Probe, Drag Coefficient.

1. Introduction

Air/Water multiphase flows occur in a wide range of natural and man-made situations. Examples include boiling heat transfer and cloud cavitation, bubble columns, cooling circuits of power plants, spraying of liquid fuel and paint, emulsions, rain, bubbles and drops due to wave breaking in the oceans, and explosive volcanic eruptions.

Attraction of multi-phase flows draws many attempts to investigate unexplored aspects of this field experimentally and numerically [1-27]. The study of flow around bodies of rectangular shape has a deep engineering interest because many civil but also industrial structure can be assimilate to this shape. From an engineering point of view, the prediction whether a structure has a potential to experience damaging vibrations or not is very important. In addition, the study of bluff body wakes and its associated fluid forces and wake frequencies is of fundamental interest. In many flow systems, complex conduits with flow obstacles have been widely employed, and the flow in them is often Air-Water. However, only a few studies of the two-phase drag experienced by such rectangular bodies have been reported in the

literature, because of its complexity and heterogeneity. Knowledge of the drag coefficient for a rectangular body, the volume fraction distribution and bubble behavior near a probe subjected to two-phase cross flow is essential for development of mechanistic understanding of fluid elastic instability of probes subjected to two-phase cross flow. The main objective of this study is to present accurate and reliable data on the combined effects of Reynolds number and volume fraction on rectangular cylinders.

1.1. Experimental Works

Many works have been performed experimentally in the field of two phase flow. In particular, Mizota & Okajima [1], using a tandem type of hot-wire probe, measured successfully flow patterns around various rectangular cylinders including a reversed flow region close to the cylinders, and confirmed that the changes of the flow patterns have close correlations with those of drag and lift forces and Strouhal numbers in the variation of the width-to-height ratio and the angle of incidence.

Yokosawa et al. [2] worked on a single tube and measured its drag coefficient under two-phase cross flow in the Reynolds numbers range of 4000-300,000 and for low void fractions (0-0.1). They found that the drag coefficient decreased with increasing volume fraction for two-phase Reynolds numbers sufficiently below the single-phase critical Reynolds number. However, for Reynolds numbers above the critical value, the drag coefficient was found to gradually increase with increasing volume fraction, although it stayed significantly less than the value for subcritical, single-phase flow. They also classified flow patterns of the two-phase wake flow behind a cylinder and to investigate quantitatively the change of the drag coefficient corresponding to the transition of the flow patterns. The former discussed the fluctuation characteristics in surface pressure, lift and drag forces on a cylinder in the two-phase or single phase cross flow.

1.2. Numerical Works

There are several numerical simulation studies for two-phase flows. For the most part, these studies addressed the case of upward flow of two-phase gas–liquid systems. But Artemiev and Kornienko [3] and Zaichik et al. [4] reported some results for downward gas–liquid flows.

Artemiev and Kornienko, developed a numeric model to predict the manner of effecting the shape of volume fraction profiles on the distribution of temperature and liquid-phase velocity in vertical flows [3]. Their model can be applied both to downward and upward flows. They investigate how gas bubbles present in the flow improve the turbulence. The turbulent viscosity was shown as a linear combination of two terms, one term being due to the liquid-phase turbulence, which the Reichardt formula can be used for its calculation, and the other term modeling the additional viscosity due to the relative gas motion. The second term has empirical constants that making the developed numerical model specified in any circumstance.

Zaichik et al. [4], proposed a diffusion-inertia model for the transport of low-inertia particles of arbitrary density. The predicted data and experimental data reported by Kamp et al. [5] were compared for gas–liquid flows in vertical pipes (the cases of downward and upward flow under various conditions of the effect due to the gravity force). In principle, it was shown to be possible to analyze bubbly flows with the help of the diffusion-inertia model, initially developed for gas-dispersed flows. The $k-\epsilon$ model of turbulence was used for single-phase flow to calculate the liquid turbulence.

A numerical model for transport phenomena in laminar upward bubbly flow was developed by Antal et al. [6]. The model was based on the Eulerian two-velocity approach. The wall force and the lifting (Saffman) force, were the major forces acting on bubbles in the laminar flow. Lopez et al. [7] reported a numerical and experimental study in which the turbulent bubbly flow in a triangular channel was analyzed. Carrica et al. [8] and Palitano et al. [9] adressed the case of poly-dispersed two-phase flows. The model makes it possible to allow for the shift of the bubble concentration maximum from the near-wall zone towards the flow core observed when the dispersed-phase size increases above some critical value. Troshko and Hassan [10] developed a numerical model involving the law of the wall for vertical mono-dispersed bubbly flow in a pipe.

In Lopez et al. [7], Carrica et al. [8], Palitano et al. [9], Troshko and Hassan [10] and Lee et al. [11] to predict the liquid-phase turbulence, a two-equation model of turbulence extended to the case of two-phase flow, was used. It can be

stated that, in spite of the intensive recent efforts aimed at numerical investigation of downward gas–liquid flows, gained data cover only a narrow range of parameters, and therefore apply only to particular conditions.

The purpose of the present study is a numerical investigation of the structure of cross Air-Water flow over selected body. A model constructed around the Eulerian representation for both phases was developed to numerically examine the structure of flow field and wake zone behind the probe in mono-dispersed Air-Water flow.

2. Nomenclature

D	Diameter (m)
F	Force (N)
K	Interphase momentum exchange coefficient
p	Pressure (Pa)
t	Time (s)
v	Velocity (m/s)
V	Volume of phase (m^3)
f	Frequency (Hz)
Re_{TP}	Two-phase Reynolds number
St	Strouhal number

Greek symbols

α	Volume fraction
μ	Dynamic viscosity $(Pa.s)$
ρ	Density (Kg/m^3)
τ	Stress-strain tensor (Pa)

Subscribe

p	primary phase
q	secondary phase

3. Numerical Approach

3.1. Eulerian-eulerian model

The different phases are mathematically interpenetrated in the Euler-Euler approach [12-16]. The concept of phasic volume fraction is introduced due to the fact that the volume of a phase cannot be taken by the other phases. Also, it is considered the volume fractions are continuous functions of space and time and their summation is equal to one. Conservation equations for each phase are derived to obtain a set of equations, which have similar structure for all phases. These equations are closed by providing constitutive relations that are obtained from empirical information or in the case of granular flows, by application of kinetic theory.

It is complicated to numerically simulate the multiphase flow using the Eulerian. It solves a set of n continuity and momentum equations for phases. Coupling through the pressure and interphase exchange coefficients, is achieved. Types of involving phases, effect on the manner in which coupling is handled; Handling of granular (fluid-solid) flows are different than non-granular (fluid-fluid) flows. Type of mixture that is modeled, affect the momentum exchange between the phases. Particle suspension, fluidized beds, bubble columns, and risers, are the applications of the Eulerian multiphase model.

3.2. Conservation of mass

The continuity phase averaged equation for phase q is:

$$\frac{\partial}{\partial t}\left(\bar{\alpha}_q \rho_q\right) + \nabla.\left(\bar{\alpha}_q \rho_q \tilde{V}_q\right) = 0 \tag{1}$$

3.3. Conservation of momentum

Neglecting laminar stress-strain tensor, gravity and other body forces, the momentum balance for phase q yields:

$$\frac{\partial}{\partial t}\left(\bar{\alpha}_q \rho_q \tilde{V}_q\right) + \nabla.\left(\bar{\alpha}_q \rho_q \tilde{V}_q \otimes \tilde{V}_q\right) = -\bar{\alpha}_q \nabla \tilde{p} + \nabla.\tilde{\tau}_q^t + F_{pq} \tag{2}$$

The tilde indicates phase-averaged variables while an over bar reflects time-averaged values. In Eq.(3) F_{pq} is the drag force between the water and air phases and can be defined as:

$$F_{pq} = K_{pq}\left[\left(\tilde{V}_p - \tilde{V}_q\right) - \left(\frac{\overline{\alpha_p' v_p'}}{\bar{\alpha}_p} - \frac{\overline{\alpha_q' v_q'}}{\bar{\alpha}_q}\right)\right] \tag{3}$$

where K_{pq} is the drag coefficient that Schiller-Nauman defined it in his study [17]. Several terms in the above equations required to be modeled to close the phase averaged momentum equations. Cokljat et al describe more about the assumptions in their analysis [18].

3.4. Geometry and grid generation

This research, for the purpose of simulating a bluff body with infinity length in a flow field, 2D geometry was opted. There are three kinds of boundary conditions in this simulation: velocity inlet, pressure outlet and wall. The top and

bottom of the channel and also boundaries of bluff body are considered as wall boundary conditions. In order to decrease errors and the effects of channel, boundaries are considered far enough from the body. The upstream length is 15 times of the face length of the rectangular probe (D), and the downstream length is 35 times of the face length. Also, top and bottom walls are considered 25D away from the center of the rectangular probe. To facilitate meshing and decrease the computational cost in numerical simulation, six rectangles around the probe which their dimensions are shown in Fig. 1 are considered as the main focus of simulation by applying finer mesh generation. To avoid unnecessary calculations, cells out of focus area with larger size have been connected to the cells of inner. Figure 1 also shows the mesh regions and the body geometry.

To make certain grid independency of the results from nodes number, for rectangular cylinder with D = 10 mm, four meshes have been tested. In Fig. 2 drag coefficients have been depicted versus different node numbers for inlet volume fraction equal to 0.2. This figure shows 230000 nodes were least nodes number which the results were totally independent of them. Therefore, it demonstrates 230000-node mesh is precise enough to capture the interests of this problem.

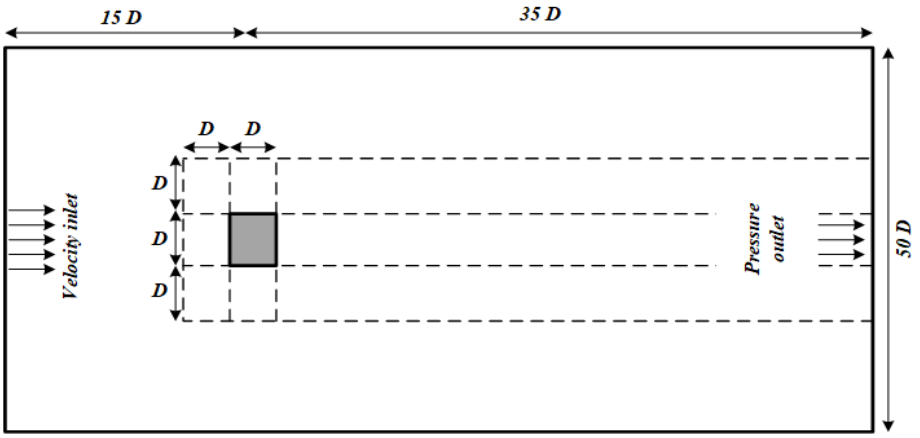

Fig. 1. Schematic of the channel and probe with the applied boundary conditions

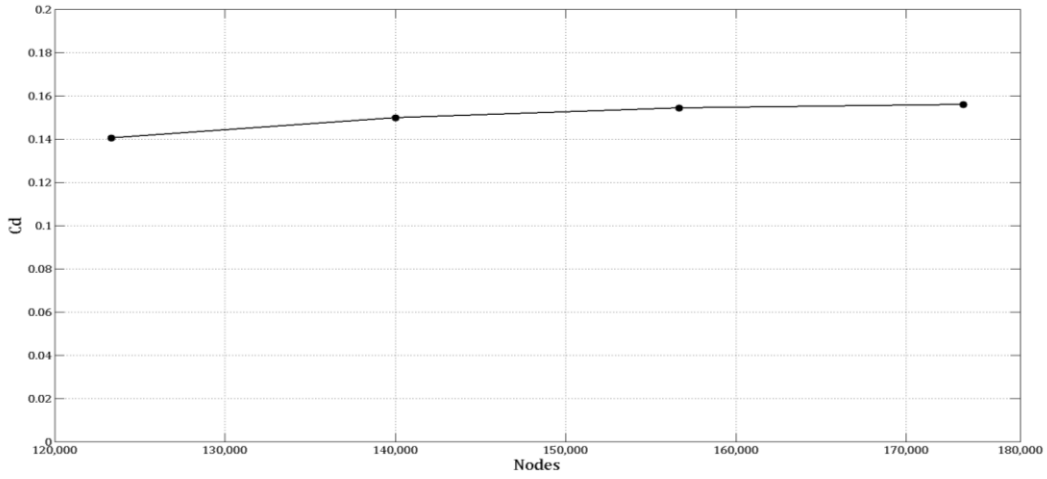

Fig. 2. Validation of mesh independency

3.5. Numerical solution method

This study utilized the method that is proposed by Mathur and Murthy, [19] and Kim et al., [20] to develop a computational method of CFD package to discretize the equations, based on the control volume frame work. Second order upwind discretization scheme is chose for discretize the governing equations. The discretized governing equation is solved using the Phase-Coupled SIMPLE (PC- SIMPLE) algorithm to couple the pressure and velocity fields. A collocated grid is used to all variables are stored at the center of control volume. The details of implementation of Reynolds-stress model into single phase were presented in Kim [21]. More details of multiphase techniques and discretization methods are found in Cokljat, [22]. To improve the stability of the numerical solution, the time dependent equations are solved. For any iteration the system of two continuity and two momentum equations with the transport equations of turbulent energy and dissipation are solved.

4. Results and discussion

The numerical simulation has been carried for the rectangular cylinder with the hydraulic diameter of 10 mm and aspect ratio of D/d = 1. At the first stage, the numerical results of drag coefficient are verified by experimental data [23]. As shown in Fig. 3 the simulation results are in good agreement with experimental data and the model can predict the overall behavior and consequently, the model has a reasonable accuracy.

In order to get a deep understanding, pressure coefficient around the obstacle was computed. Figure 4 shows the start point and the direction of the curve length schematically.

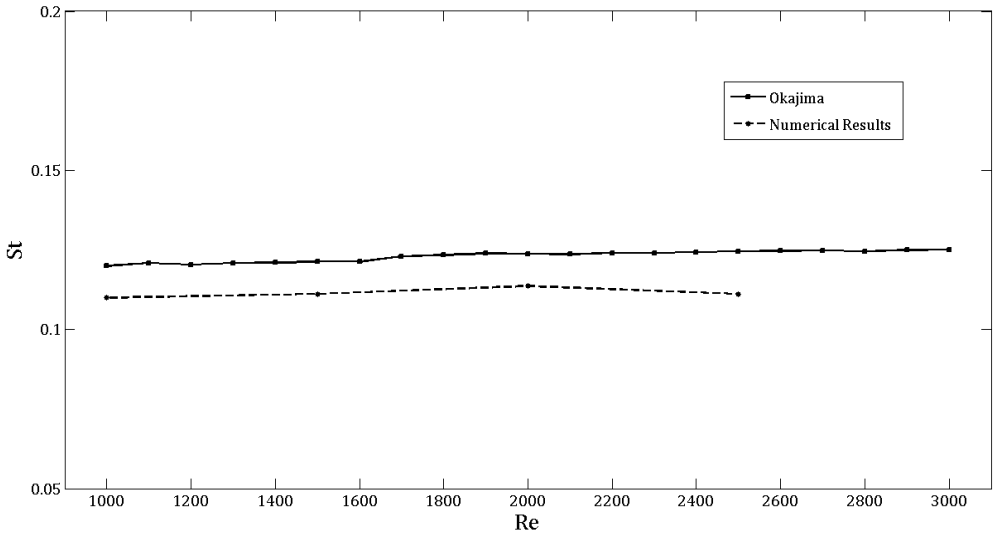

Fig. 3. Comparison between the experimental results and the present work

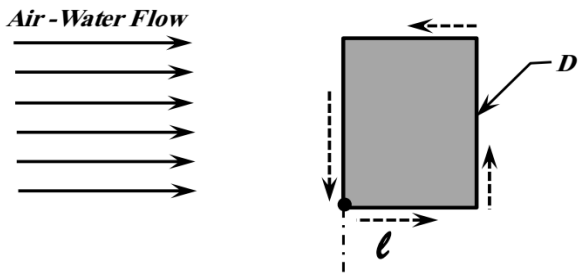

Fig. 4. Schematic curve length

In Fig. 5 the curve shows the variation of pressure coefficient along curve length for $Re = 1000$ and $\alpha = 0.1$. At the stagnation point, pressure coefficient has its maximum value, and it is seen on the bottom and top faces there are abrupt changes in the pressure coefficient due to appearance of wake effects.

Figure 6 illustrates the variation of drag coefficient versus Reynolds number for the cylinder in inlet air volume fraction of 0.1 to 0.5. This figure depicts increase of volume fraction which represent more portion of second phase can decrease the total drag force on the cylindrical body. It also demonstrates along Reynolds number axis, it is not apparent difference in drag coefficient among the various volume fractions.

The liquid phase is water and gas phase is air which the range of volume fraction varies from 0.01 to 0.5, also diameters of bubbles at inlet were considered 1 mm. Moreover Re_{TP} is in the range of 1000 – 3000, which is defined by:

$$Re_{TP} = \frac{\left(\alpha\rho_g + (1-\alpha)\rho_f\right)vD}{\left(\alpha\mu_g + (1-\alpha)\mu_f\right)} \tag{4}$$

and

$$St = \frac{fD}{v} \tag{5}$$

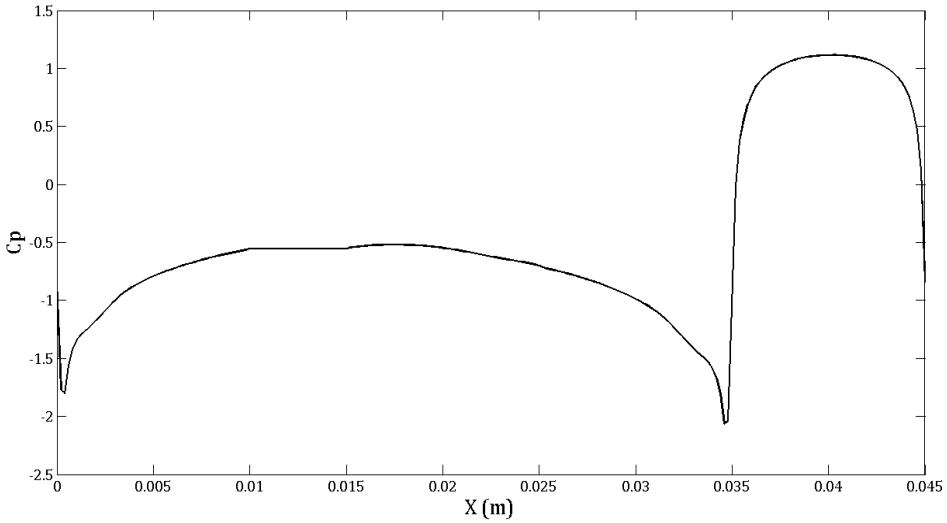

Fig. 5. The variation of the pressure coefficient along the length of the curve at Reynolds number of 1000 and volume fraction 0.1

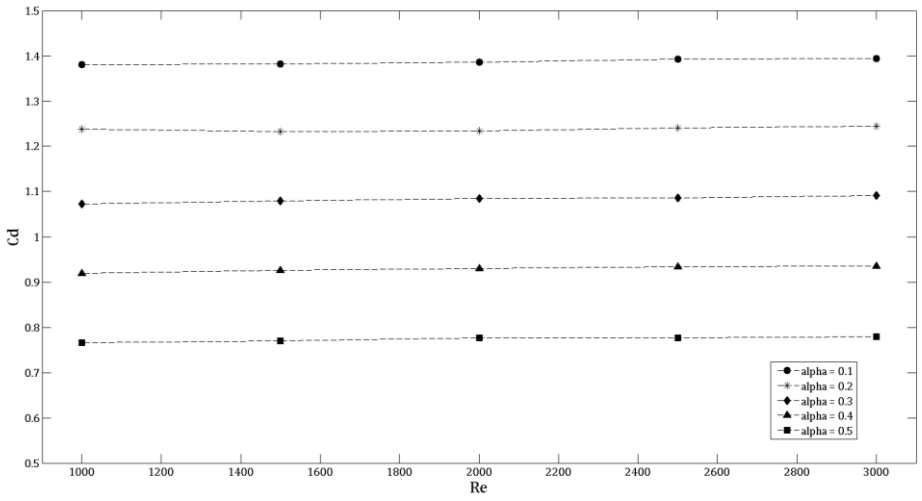

Fig. 6. Variation of C_d versus Re for air volume fractions

To calculate Strouhal number based on Eq.(5) frequency of vortex shedding must be obtained. Thus, as a reference to obtain frequency of oscillating flow, diagram of drag coefficient in flow time was used. Figure 7 demonstrates one of period of drag coefficient waves for this mechanism in which frequency of this vortex can be easily calculated.

The Fig. 8 shows the variation of Strouhal number versus alpha and Reynolds number. It shows that inlet volume fraction has a direct relation with the Strouhal number. As a result of rising frequency of vortex shedding by increasing Reynolds number, the magnitude of Strouhal numbers increases and there is a critical Reynolds number around 2600 which causes huge jump in Strouhal number independent of volume fraction.

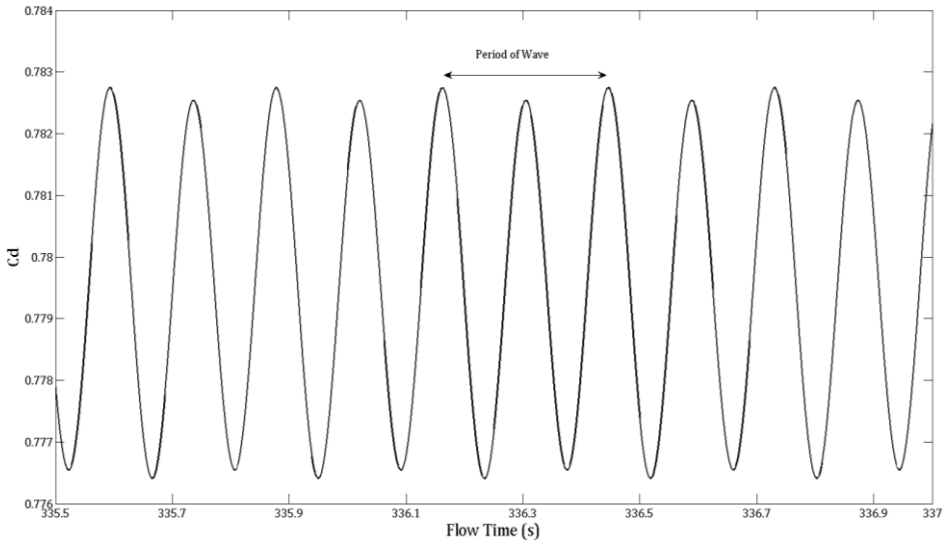

Fig. 7. Drag coefficient in flow time

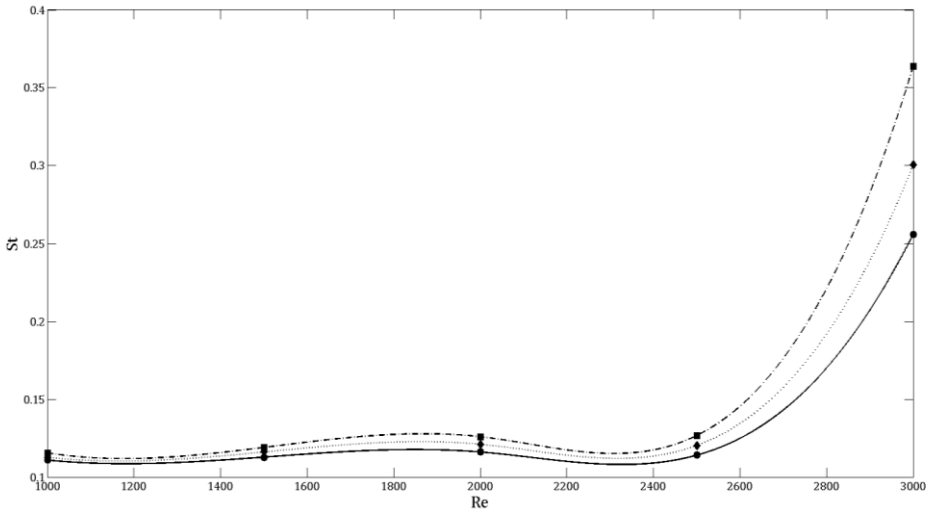

Fig. 8. Strouhal number versus Re for various volume fractions including alpha = 0.1 (black line), 0.3 (dotted line), and 0.5 (dashed line)

5. Conclusion

In this article, a numerical approach is used to investigate drag and pressure coefficient for rectangular cylinder in air- water two-phase flow. The current data compared with experimental data to validate the numerical simulation. It is shown the effects of wake on pressure coefficient along curve length and the results show the overall behavior of pressure coefficient is the same as single phase flow. Also, it was illustrated the inverse relation between drag coefficient and volume fraction in this problem. To draw a conclusion, the perception of calculations of Strouhal numbers for various Reynolds number conveys that there is abrupt change in Strouhal number after $Re_{Critical} = 2600$ independent of volume fraction of inlet flow.

References

[1] Okajima A., Sugitani K., Mizota T., Flow Around a Pair of Circular Cylinders Arranged Side by Side at High Reynolds Numbers, Transactions of the JSME (1986) 52 (480): 2844-2850.

[2] Yokosawa M., Kozawa Y., Inoue A., Aoki S., Studies on Two-Phase Cross Flow, Part II: Transition Reynolds Number and Drag Coefficient, International Journal of Multiphase Flow (1986) 12(2)169-184.

[3] Artemiev V. K., Kornienko Yu. N., Numerical Modeling of Influence Non-Monotonic Profile of Gas (vapor) Content on a Distribution of Velocity and Temperature in a Two-Phase Bubbly Flow, Proceedings, 3rd Russian National Conference on Heat Transfer, Moscow, Russia (2002)5:41–44.

[4] Zaichik L. I., Skibin A. P., Soloviev S. L., Simulation of the Distribution of Bubbles in a Turbulent Liquid Using a Diffusion-Inertia Model, International Journal of High Temp (2004) 42:111–118.

[5] Kamp A., Colin C., Fabre J., The Local Structure of a Turbulent Bubble Pipe Flow under Different Gravity Conditions, Proceedings, 2nd International Conference on Multiphase Flow, Kyoto, Japan (1995) 3(P6).

[6] Antal S. P., Lahey Jr. R. T., Flaherty J. F., Analysis of Phase Distribution in Fully Developed Laminar Bubbly of Two-Phase Flow, International Journal of Multiphase Flow (1991)17:363–652.

[7] Lopez M. A., Lahey Jr. R. T., Jones O. C., Phase Distribution in Bubbly Two-Phase Flow in Vertical Ducts, International Journal of Multiphase Flow (1994) 20: 805–818.

[8] Carrica P. M., Drew D. A., Bonetto F., Lahey Jr. R. T., A Polydisperse Model for Bubbly Two-Phase Flow Around Surface Ship, International Journal of Multiphase Flow (1999) 25:257–305.

[9] Politano M. S., Carrica P. M., Converti J., A Model for Turbulent Polydisperse Two-Phase Flow in Vertical Channel, International Journal of Multiphase Flow (2003)29: 1153–1182.

[10] Troshko A. A., Hassan Y. A., A Two-Equation Turbulence Model of Turbulent Bubbly Flow, International Journal. of Multiphase Flow (2001) 27: 1965–2000.

[11] Lee S. L., Lahey Jr. R. T., Jones O. C., The Prediction of Two-Phase Turbulence and Phase Distribution Phenomena Using a $k-\epsilon$ Model, Japan Journal of Multiphase Flow (1989)3: 335–368.

[12] Simonin, C., Viollet, P.L., Predictions of an Oxygen Droplet Pulverization in a Compressible Subsonic Coflowing Hydrogen flow, Numerical Methods for Multiphase Flows (1990) 91: 65–82.

[13] Cokljat D., Slack M., Vasquez S.A., Bakker A., Montante G., Reynolds-Stress Model for Eulerian multiphase, Progress in Computational Fluid Dynamics, An International Journal (2006) 6(1/2/3): 168 – 178.

[14] Mathur S.R., Murthy J.Y., A Pressure Based Method for Unstructured Meshes, Numerical Heat Transfer (1997)31:195–216.

[15] Okajima A., Strouhal Numbers of Rectangular Cylinders, The Journal of Fluid Mechanics (1982)123: 379-398.

[16] Norberg C., Flow Around Rectangular Cylinders, Pressure Forces and Wake Frequencies, Journal of Wind Engineering and Industrial Aerodynamics (1993) 49: 187-196.

[17] Schiller L., Naumann Z., A Drag Coefficient Correlation (1935) 77: 318.

[18] Cokljat D., Ivanov V.A., Sarasola F.J., Vasquez S.A., Multiphase K-Epsilon Models for Unstructured Meshes, ASME Paper FEDSM2000-11282, Proceedings of ASME FEDSM 2000: Fluids Engineering Division Summer Meeting, Boston USA.

[19] Mathur S.R., Murthy J.Y., A Pressure Based Method for Unstructured Meshes, Numerical Heat Transfer (1997)31:195–216.

[20] Kim S.E., Mathur S.R., Murthy J.Y., Choudhury D., A Reynolds-Averaged Navier-Stokes Solver Using Unstructured Mesh-Based Finite-Volume Scheme, AIAA (1998) 98-0231.

[21] Kim S.E., Unstructured Mesh Based Reynolds Stress Transport Modeling of Complex Turbulent Shear Flows, AIAA (2001) 2001-0728.

[22] Cokljat D., Slack M., Vasquez S.A., Bakker A., Montante G., Reynolds-Stress Model for Eulerian multiphase, Progress in Computational Fluid Dynamics, An International Journal (2006) 6(1/2/3):168 – 178.

[23] Okajima A., Strouhal Numbers of Rectangular Cylinders, The Journal of Fluid Mechanics (1982) 123(1982): 379.

[24] Fabio Toshio K., Ribatski G., Void Fraction and Pressure Drop during External upward Two-Phase Crossflow in Tube Bundles–Part I: Experimental Investigation, International Journal of Heat and Fluid Flow 65 (2017): 200-209.

[25] Fabio Toshio K., Ribatski G., Void Fraction and Pressure Drop during External upward Two-Phase Crossflow in Tube Bundles–Part II: Predictive Methods, International Journal of Heat and Fluid Flow 65 (2017): 210-219.

[26] Hojati A., Hanafizadeh P., Effect of Inclination Pipe Angle on Oil-Water Two Phase Flow Patterns and Pressure Loss, In Proceedings of the Biennial Conference on Engineering Systems Design and Analysis ESDA2014, Copenhagen, Denmark (2014).

[27] Ghanbarzadeh S., Hanafizadeh P., Saidi M.H., Bozorgmehry R., Fuzzy Clustering of Vertical Two Phase Flow Regimes Based on Image Processing Technique, In Proceedings of the ASME 3rd Joint US-European Fluids Engineering Summer Meeting (2010) 303-313.